

CONDITIONS FOR SQUARE HYSTERESIS LOOPS IN FERRITES

by H. P. J. WIJN, E. W. GORTER, C. J. ESVELDT and P. GELDERMANS.

538.23:621.318.134

Since ferrites were introduced commercially by Philips nearly ten years ago, the applications of these soft magnetic materials have enormously increased. The further development of these materials has been influenced by the fact that it has been found possible to manufacture them with properties specially adapted to particular purposes. The present article deals with the fundamental conditions for obtaining ferrites with rectangular hysteresis loops.

Introduction

Magnetic cores with approximately rectangular hysteresis loops have a wide range of application. They are used for example in the so-called "magnetic memory"¹⁾ of computing machines and automatic pilots, and for magnetic switching elements.

For a memory element, the requirements are that when a square pulse of a certain height is passed through the magnetizing coil, the core shall revert to its original condition after passage of the pulse but when a pulse of *double* this height is passed through the coil, the magnetization of the core shall be *reversed* after passage of the pulse. When the material is used for switching elements, the magnetization must not be affected by a positive pulse, but must be reversed by a negative pulse of the same height.

The pulses employed in these techniques are usually of very short duration, so that, during the pulse, the variation in the current, di/dt , assumes very high values, as a result of which rapid variations dB/dt occur in the induction, and eddy currents are produced.

It is important that the magnitude of these eddy currents should be minimized. In ferromagnetic metals (nickel-iron alloys such as "Hypernik" and "Deltamax"²⁾) this is to a limited extent achieved by building up the core from very thin insulated laminations of the material; in practice, however, it is difficult to construct such laminated cores to give nearly rectangular hysteresis loops.

Magnetically soft materials such as ferrites³⁾,

¹⁾ J. A. Rajchman, RCA rev., **13**, 183-201, 1953. A. Wang, J. appl. Phys. **21**, 49-54, 1950. Some specific instances are reviewed in F. van Tongerloo, T. Nederlands Radiogenootschap **18**, 265-285, 1953, No. 11.

²⁾ See for example R. M. Bozorth, Ferromagnetism, Van Nostrand, New York, 1952.

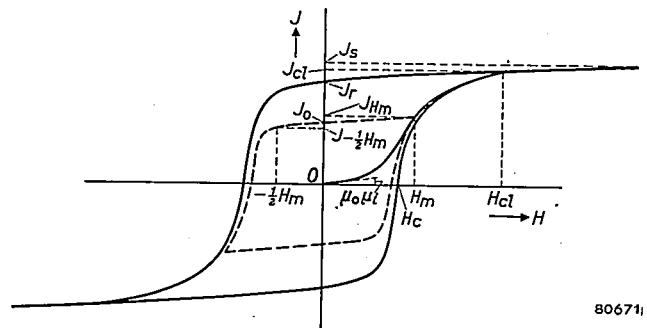
³⁾ J. L. Snoek, Philips tech. Rev. **8**, 353, 1946; J. J. Went and E. W. Gorter, The magnetic and electrical properties of Ferroxcube materials, Philips tech. Rev. **13**, 181-193, 1951/1952, referred to hereafter as I. As in I, the present article uses the rationalized Giorgi (M.K.S.) system, in which B is measured in Wb/m^2 and H in A/m ($\mu_0 H$ in Wb/m^2). $B = 10^{-4} \text{ Wb/m}^2$ corresponds to $B = 1$ gauss, and $\mu_0 H = 10^{-4} \text{ Wb/m}^2$ ($H = 79.5 \text{ A/m}$) to $H = 1$ oersted. $\mu_0 = 4\pi \times 10^{-7}$ volt seconds/ampere metres. The formula $B = \mu_0 H + J$ takes the place of $B = H + 4\pi I$ in the electromagnetic c.g.s. system. If $J = 1 \text{ Wb/m}^2$, $4\pi I = 10,000$ gauss and $I \approx 800$ gauss.

which are at the same time poor conductors, offer considerable advantages over the use of laminated ferromagnetic metals in pulse applications (given that these materials can be made with rectangular hysteresis loops⁴⁾).

Definitions of certain quantities

One or two concepts will now be introduced which are essential to a consideration of the problem⁵⁾.

The loop depicted in *fig. 1* (full line) is the hysteresis loop of a ferrite. It represents the magnetization J plotted against the magnetic field H for values



80671

Fig. 1. Hysteresis loop of a ferrite.

of H which decrease from large positive to large negative values, and then revert to the positive value. The value of the field at which the magnetization is zero is known as the coercive force H_c of the material⁶⁾. On decreasing the field from a large value, the point at which the magnetization

⁴⁾ E. Albers-Schoenberg and D. R. Brown, Electronics **26**, April 1953, p. 146.

⁵⁾ For a more detailed discussion of these concepts and their physical basis see J. J. Went, Philips tech. Rev. **10**, 246-254, 1948/1949.

⁶⁾ In magnetic materials a distinction is made between a coercive force for the induction, BH_c , i.e. the field strength at which the induction B is zero, and a coercive force for the magnetization, JH_c , the field strength at which the magnetization J is zero. In general, BH_c and JH_c differ because $B = \mu_0 H + J$, and B and J do not become zero at the same time. In the materials discussed here the values of H are so small that the difference may be disregarded and the single symbol (H_c) employed.

begins to diverge from its previous values is denoted H_{cl} ; the corresponding magnetization is denoted J_{cl} . For fields $H > H_{cl}$ the variations in the magnetization are reversible. Smaller hysteresis loops are also obtainable, as shown for example by the dotted line in fig. 1, with extreme field values of $+H_m$ and $-H_m$ ($H_m < H_{cl}$). As a measure of the effectiveness of ferrites for the cores of memory devices the concept of "squareness" is introduced, defined as:

$$R_s = \frac{B_{-\frac{1}{2}H_m}}{B_{H_m}}$$

or, what is practically equivalent,

$$R_s = \frac{J_{-\frac{1}{2}H_m}}{J_{H_m}} \dots \dots \dots (1)$$

The demoninator and numerator of the latter represent respectively the magnetization for a field $+H_m$ and that for a field $-\frac{1}{2}H_m$. It will be clear that R_s is also a function of the maximum field H_m determining the size of the loop. When R_s is measured as a function of H_m it is found that a maximum occurs for a certain value of H_m ; let this maximum be denoted by $(R_s)_{max}$. With ferrites for which $(R_s)_{max} > 0.7$, this value of H_m is roughly equal to H_c .

When ferrites are employed as switching elements the ratio J_0/J_{H_m} is important; J_{H_m} represents the above mentioned magnetization for a field H_m , and J_0 the remanent magnetization after removal of the field (see fig. 1). J_0/J_{H_m} is a function of H_m , and the maximum, $(J_0/J_{H_m})_{max}$, of this ratio is also of interest.

General considerations

Magnitude of the remanent magnetization

Consider as the starting point the demagnetized condition, that is, point O in fig. 1. It may be taken as generally known that in this condition the material is divided up into "Weiss domains" within which the material is uniformly magnetized (see ⁵). The magnetization vector in each of these Weiss domains lies in a certain direction (the preferential direction) and the magnetization averaged over all the domains is zero. The preferential direction of magnetization in each domain is determined by three factors, namely the crystal anisotropy, the stress anisotropy and the shape anisotropy. These factors will be discussed presently. Very small external magnetic fields turn the magnetization vectors away from their preferential orientation, towards the direction of the applied field. The extent

to which this is possible in the case of sintered ferrites is represented approximately by the quantity μ_i , the initial permeability ⁷) (see fig. 1).

When the material is magnetized by a very strong field, all the magnetization vectors are parallel to each other and there is no longer any division into Weiss domains. This corresponds to the saturated state with magnetization J_s (see fig. 1). If the field be now gradually reduced to zero, the magnetization vectors turn from the direction of the field towards the nearest preferential directions as determined by the anisotropies mentioned above.

When the field H is zero a magnetization J_r remains (the remanence). For an ideal rectangular loop $J_r/J_s = 1$. If H be varied slightly, starting from the remanent state, a permeability μ_{rem} will be found which is again determined by the rotation of the magnetization vectors. The magnitude of the ratios J_r/J_s and μ_{rem}/μ_i , corresponding to the three kinds of anisotropy, will now be evaluated. The significance of the second of these ratios will appear later.

a) Crystal anisotropy. In nearly all cubic ferrites it has so far been found that the body diagonal is the preferential direction of the magnetization; there are accordingly eight such preferential directions. The magnetization energy per unit volume of a material whose magnetization vector is defined by the direction-cosines (with respect to the cubic axes) a_1 , a_2 and a_3 , is given to a first approximation by:

$$E = K(a_1^2 a_2^2 + a_1^2 a_3^2 + a_2^2 a_3^2) \dots (2)$$

In this expression, K may be both positive and negative. In materials with positive K , the value of E is at a minimum when one a is equal to unity and the others are zero, that is, when the magnetization vector is parallel to one of the sides of the cube.

In most ferrites, however, and also in some metals such as nickel, K is negative. E is then at a minimum when the factor between brackets in (2) is at a maximum, viz. when $a_1 = a_2 = a_3$. The magnetization vector is then parallel to one of the body diagonals of the cube. If the crystal anisotropy is the only anisotropy present, when the field is reduced to zero after saturation in a strong field, the magnetization vectors of the Weiss domains in polycrystalline materials turn back from the direction of the field to the nearest cube diagonal (a (111)-direction).

⁷) In contrast with article I, μ_i is taken as the relative permeability. The corresponding absolute permeability is $\mu_0 \mu_i$, for which the symbol μ_i was used in I. The same applies to the quantity μ_{rem} introduced later.

Since there are eight preferential directions, the vectors revert to directions which are all contained within the solid angle $\pi/2$ (fig. 2). According to calculations by Gans ⁸⁾, this leads to $J_r/J_s = 0.87$ and $\mu_{rem}/\mu_i = 0.36$.

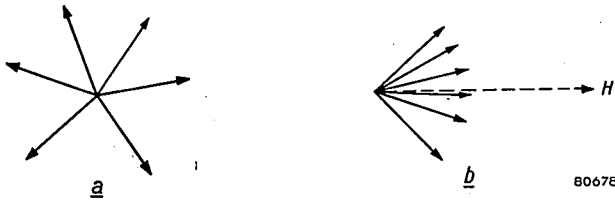


Fig. 2. a) Distribution of the magnetization vectors in the Weiss domains in demagnetized polycrystalline materials. b) As above for the remanent state when (negative) crystal anisotropy predominates.

b) *Stress anisotropy.* It is well-known that the length of a rod of magnetic material changes with its magnetization; this property is known as magnetostriction. A distinction is made between positive and negative magnetostriction according to whether the magnetization is accompanied by an expansion or a contraction in the direction of magnetization.

If strains are present in the material as a result of elastic deformation, the magnetization tends to be so oriented that the accompanying variations in length oppose these strains. If the stress anisotropy predominates there will be only two preferential directions for the magnetization at every point in the material. In the case of negative magnetostriction (as usually found in ferrites), these directions correspond at each point to the two orientations at which the magnetization vectors are parallel to the greatest compressive strain or the smallest tensile strain. Here, too, the magnetization vectors turn back to the nearest preferential direction when the field is reduced to zero from the saturation value. For a random distribution of the strains in the material the vectors revert to preferential directions distributed over a solid angle of 2π (see fig. 3b). Under these conditions it has been calculated that $J_r/J_s = 0.5$.

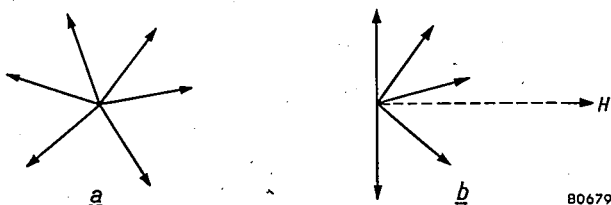


Fig. 3. a) As fig. 2a. b) Distribution of the magnetization vectors for the remanent state when stress anisotropy predominates.

For ferrites with small crystal anisotropy but with a large magnetostriction coefficient, it is possible, when sufficiently large external forces are applied, that the latter determine the preferential direction of the magnetization. This has been demonstrated in the Eindhoven Laboratory by G. W. Rathenau and G. W. van Oosterhout in the following manner. A ring of glass was melted onto the outer cylindrical surface of a ring of Ferrocube ⁹⁾. The coefficient of expansion of the glass was slightly higher than that of the Ferrocube, so that after cooling to room temperature the Ferrocube was subjected to tangential compression. The magnetization caused by the negative magnetostriction was therefore parallel to the predominant strain. Consequently the strains in the ferrite were no longer distributed in a random manner, but mainly in one direction only, so that at every point in the material only two orientations of the magnetization were possible, viz. parallel and anti-parallel to the strain. The remanence after removal of a field parallel to the compression (i.e. a tangential field) can thus theoretically assume a value equal to the saturation magnetization $J_r/J_s = 1$. Fig. 4 shows a family of hysteresis loops plotted

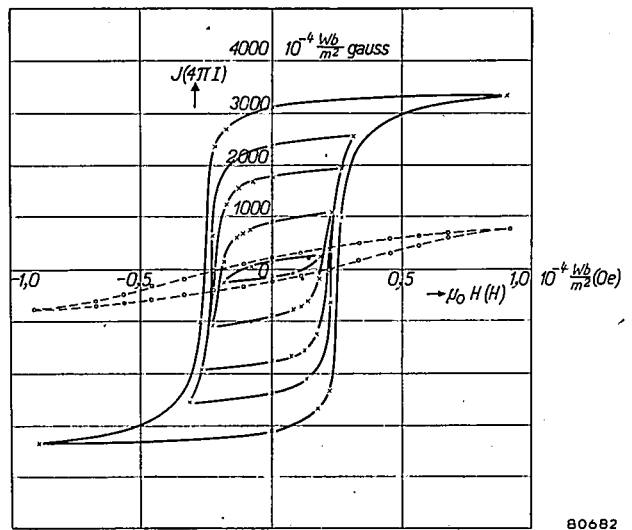


Fig. 4. Family of hysteresis loops for a ring of Ferrocube IVA enclosed by a band of special glass. Dashed curve: hysteresis loop for Ferrocube IVA without glass (see text).

from measurements on a ring of Ferrocube IVA enclosed in glass. The loop drawn in broken lines is that of the ring without the glass. A great advantage of this type of material, with its rectangular hysteresis loop, is the low coercive force.

⁸⁾ R. Gans, Ann. Physik 15, 28, 1932.

⁹⁾ Netherlands Patent application No. 175120, dated Jan. 1953.

Similar results have been obtained by enclosing a ferrite ring in synthetic resin¹⁰).

If a polycrystalline material, prepared in the demagnetized state (O , fig. 1) by cooling from a temperature above the Curie point, contains no strain the direction of the magnetization vector in each Weiss domain is determined by the crystal anisotropy (disregarding shape anisotropy, see c). The magnetization vectors of the Weiss domains are then oriented in the above-mentioned preferential directions. When the material is magnetized and then brought into the remanent state, a large number of the individual magnetization vectors are turned from their original preferential direction into another. In general, this will be accompanied by a change of shape of individual crystals. For example, if the body diagonals are the preferential directions in cubic ferrites, the length of the body diagonal will depend on whether the magnetization vector is parallel to this diagonal or not. The corresponding difference in length is called the "magnetostriction in the preferential direction", λ_{111} . Even if there is no strain present in a polycrystalline material in the demagnetized state, there may nevertheless be strains present in the remanent state, unless $\lambda_{111} = 0$. In this particular case, the magnitude of the remanence is determined by the crystal anisotropy only: this is a requirement for high remanence¹¹).

The results of measurements on a series of mixed crystals of nickel ferrite and ferrous ferrite shows the importance of magnetostriction in the pre-

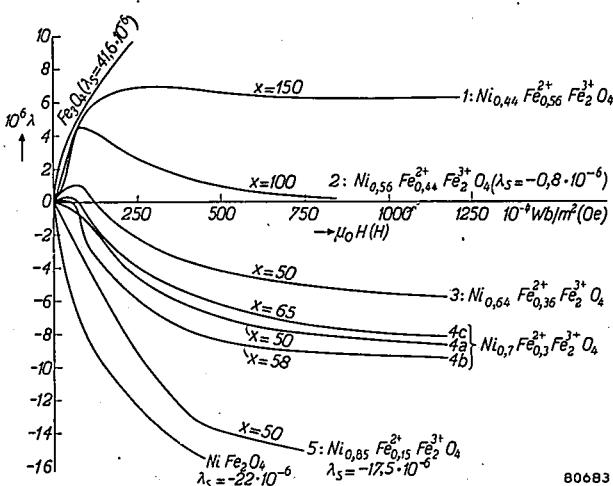


Fig. 5. Magnetostriction as a function of the magnetic field in polycrystalline samples of mixed crystals of nickel ferrous ferrite. All samples were fired at 1350°C, but in gas currents of different composition, viz. 600 ml/min $\text{CO}_2 + x$ ml/min of a mixture of 90% N_2 and 10% H_2 . The value of x and the chemical composition of the ferrites are shown in respect of each curve.

¹⁰) H. J. Williams, R. C. Sherwood, Matilda Goertz and F. J. Schnetler, Commun. Electr. 9, 531, 1953.

¹¹) For these considerations we are indebted to J. Smit of the Eindhoven Laboratory.

ferential direction. Fig. 5 shows the magnetostriction λ plotted against the magnetic field H for polycrystalline preparations of mixed crystals of Fe_3O_4 and NiFe_2O_4 . The saturation magnetostriction (the value of λ for effective saturation) of these materials is $+41.6 \times 10^{-6}$ and -22×10^{-6} respectively, so that it may be expected to

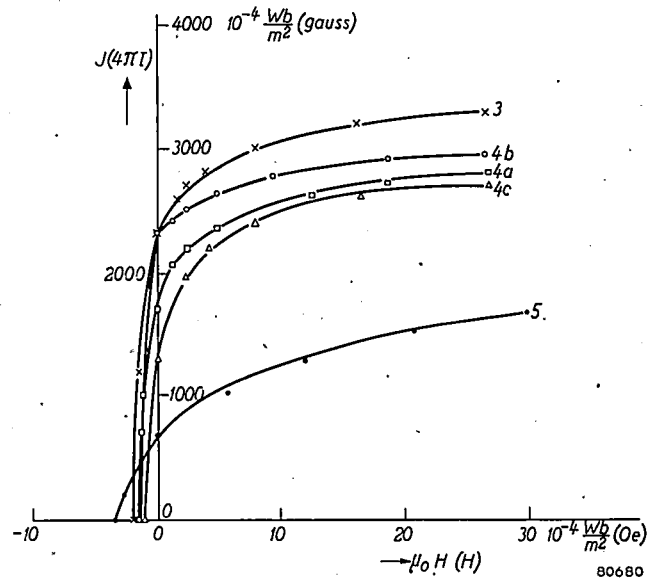


Fig. 6. Upper branch of the hysteresis loop for decreasing fields, for some of the ferrites in fig. 5.

be zero for a mixed crystal with a certain ratio of these constituents. It is, in fact, seen from fig. 5 that the saturation magnetostriction λ_s of $\text{Ni}_{0.56}\text{Fe}_{0.44}\text{Fe}^{2+}\text{Fe}^{3+}\text{O}_4$ is very small ($\lambda_s = -0.8 \times 10^{-6}$). It was shown earlier, however, that it is the magnetostriction in the preferred direction that must be small in order to obtain a rectangular hysteresis loop. It can be shown quite simply that the sign of the magnetostriction of a specimen in a field of the same order of magnitude as the coercive force (i.e. $\mu_0 H_c \approx 10^{-4} \text{ Wb/m}^2$, $H_c \approx 1$ oersted, for mixed nickel-ferrous-ferrites) is the same as the sign of the magnetostriction in the preferred crystallographic direction. Fig. 5 shows that the sign of the preferential magnetostriction is reversed in compositions occurring between those of samples 4a and 4b ($\text{Ni}_{0.7}\text{Fe}_{0.3}\text{Fe}^{2+}\text{Fe}^{3+}\text{O}_4$ fired at 1350 °C in a current of gas consisting of 600 ml carbon dioxide and x ml nitrogen with 10% hydrogen, per minute¹²)).

Part of the hysteresis loops of a number of the ferrites referred to in fig. 5 are shown in fig. 6. It

¹²) The difference in the reducing power of these gases results in a slight displacement in the ratio of Ni^{2+} to Fe^{2+} in the ferrite. The quantity of NiO or FeO that may occur as second phase can be disregarded, in comparison with the volume of the pores.

can be seen that samples 4a and 4b do actually yield the anticipated greater squareness compared with the other materials.

c. Shape anisotropy. It is well known that when an open magnetic circuit is magnetized an opposing field is produced, i.e. partial demagnetization occurs, due to the "free poles" at the extremities. This opposing field, which may be regarded as due to shape anisotropy, is proportional to the magnetization. Although this article is concerned only with magnetic circuits which can be considered macroscopically as closed, we are nevertheless to a large extent concerned with demagnetization due to shape anisotropy in view of the more or less porous structure of the ferrite (see fig. 10). The porosity of the sintered material varies between 1% and about 25%, and the effect of the air inclusions is such that the field H_{int} in the material is weaker than the applied field H_{ext} . In general it can be said that this difference is proportional to the magnetization of the material:

$$\mu_0(H_{\text{ext}} - H_{\text{int}}) = NJ \dots (3)$$

where N is a constant depending on the porosity.

In consequence of this, the measured hysteresis loop differs from that which would be obtained if the material were free from cavities or pores (see fig. 7). This effect can be regarded as a "shearing" of the

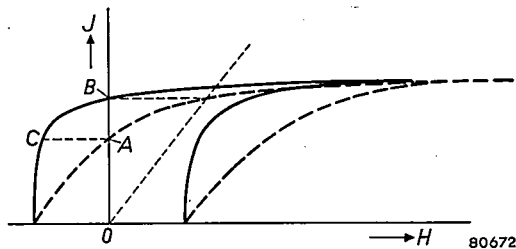


Fig. 7. Effect of "shearing" in the apparent shape of the hysteresis loop.

hysteresis loop. It will be seen from the figure that, owing to the shearing, the ratio J_r/J_s is considerably reduced, since J_r decreases whilst J_s of course remains constant. It may be noted that in the absence of shearing, the state corresponding to the point B is typified by a distribution of the magnetization vectors as in fig. 2b or 3b, according to which kind of anisotropy predominates. When shearing occurs, the point A is only apparently the remanent state; in fact the material is in a demagnetizing field $\mu_0 H = -NJ$, so that the actual state of the material is as shown at C . The distribution of the vectors is now very different from that in figs. 2b and 3b, and more resembles that of the demagnetized

condition (figs. 2a and 3a). It is also to be expected that μ_{rem}/μ_i will now be more nearly equal to unity, even in the case of predominant crystal anisotropy. In ferrites with equal saturation magnetization J_s and with similar porosity (i.e. equal N), the smaller the coercive force of the ferrite, the greater the influence of the demagnetizing field on the hysteresis loop.

Of possibly greater importance than the "shearing" is the effect of the porosity on the preferential direction of the magnetization at every point in the material. It is to be expected that in porous materials the direction of magnetization at each point will be largely determined by the direction of the demagnetizing field at the point. These demagnetizing fields result in only one preferred direction at each point, so that a low value of J_r/J_s may be anticipated.

To obtain "rectangular" hysteresis loops, the ratio J_r/J_s should be as nearly as possible equal to unity. With polycrystalline materials this can best be approximated when the crystal anisotropy predominates over the other anisotropies. It is especially important to ensure that shape anisotropy is absent: this means that porosity must be as low as possible. It is then found that $J_r/J_s = 0.87$. Higher values could be obtained if it were possible to ensure that the crystals are so oriented that all their body diagonals are parallel; this could even yield $J_r/J_s = 1$. This possibility cannot be pursued further here.

The coercive force

From the point of view of the application of ferrites with rectangular hysteresis loops it is important that the coercive force H_c shall be as small as possible. This is because H_c determines the number of ampere-turns necessary to reverse the direction of the remanent magnetization in the core. The coercive force is related to the field strength needed to displace the boundaries between the Weiss domains i.e. the Bloch walls. These "walls" are fixed at certain locations in the material as a result of internal strains and non-magnetic inclusions. It is to be expected that such walls in ferrites will be fixed to air pores which usually occur in a far greater number than in metals. We may therefore, for a moment, consider Néel's theory¹³⁾, which gives an insight into the effect of porosity on the magnitude of H_c . Néel points out the fact that the internal stray magnetic fields caused by inclusions in ferromagnetic materials

¹³⁾ L. Néel, Ann. Univ. Grenoble, 22, 299-343, 1946, and Physica 15, 225-234, 1949.

are limited to smaller domains when the Bloch walls pass through the inclusions. This is illustrated in *figs. 8a* and *b*. The magnetic "charges" of opposite sign are closer to each other in *b* than in *a*, which

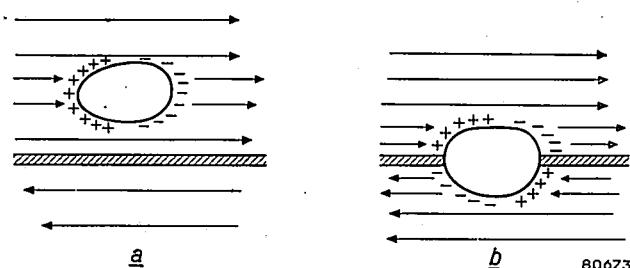


Fig. 8. Effect of inclusions or pores on the energy in a Bloch wall (Néel¹³)

a) wall not intersecting the cavity.
b) wall intersecting the cavity.

means that the total magnetic energy is considerably less in *b* than in *a*. The location of the Bloch walls at which minimum free energy occurs is

where p represents the porosity of the material¹⁴).

The relationship between p and H_c in the range of Ni-Zn ferrites of differing properties has been investigated experimentally (see *Table I*), and the value of H_c , as computed from formula (4), is shown in the last but one column, $|K|$ being calculated from μ_i on the assumption that μ_i is determined only by rotation (i.e. $\mu_i - 1 = \frac{1}{2} J_s^2 / \mu_0 |K|$). It is seen that in the range of porosities considered, H_c does depend on the porosity.

If a low value of H_c is to be attained, the ferrite must be well sintered during preparation to obtain as low a porosity as possible. This can be achieved by firing at a high temperature, by employing a ferrite having a relatively low melting point, or by adopting a suitable ceramic technique. In the last two instances a high temperature is avoided, thus minimizing chemical reduction of the ferrite with its adverse consequences on the magnetic and electrical properties.

Table I. Relation between porosity and coercive force of nickel-zinc ferrites.

Ferro-cube IV Type	Firing temp. °C	Chemical composition in mole % (remainder FeO + Fe ₂ O ₃)		Porosity p %	Saturation magnetization		Initial permeability μ_i	Coercive force $\mu_0 H_c : 10^{-4}$ Wb/m ² H_c : oersted	
		NiO	ZnO		J_s 10 ⁻⁴ Wb/m ²	J_s gauss		per Eq. (4)	measured
A	1250	17.5	33.2	8.9	3650	292	650	0.4	0.4
B	1250	24.9	24.9	15.4	4150	332	230	2.0	1.4
C	1250	31.7	16.5	22.5	4012	321	90	6.2	4.0
D	1250	39.0	9.4	24.3	3537	283	45	10.4	6.8
E	1250	48.2	0.7	24.8	2450	196	17	16.1	13.7
A	1450	17.5	33.2	9.5	3620	290	470	0.6	0.3
B	1450	24.9	24.9	3.2	4750	380	312	0.4	0.4
C	1450	31.7	16.5	8.0	4760	381	86	2.7	1.1
D	1450	39.0	9.4	8.9	4260	341	63	3.5	1.7
E	1450	48.2	0.7	9.9	1688	135	42	3.7	3.2

therefore that at which the wall intersects as many air pores as possible. The coercive force is then the field strength necessary to dissociate a wall from its air pores, and this coercive force will be related to the concentration, as well as to the size, of the air pores. It has been found that inclusions or pores of diameters comparable to the Bloch wall thickness exercise the greatest influence on H_c . According to Néel's theory, the coercive force H_c in the case of negative crystal energy (K negative), when the absolute value of K is high compared with J_s^2 / μ_0 (which applies to the ferrites considered here), is given by the formula:

$$H_c = \frac{4|K|p}{3\pi J_s} \left[0.39 + \frac{1}{2} \ln \frac{3J_s^2}{4\mu_0 |K|} \right], \quad (4)$$

High remanence and small coercive force

Let us now briefly summarise the conditions to be fulfilled in order to obtain materials with square hysteresis loops (i.e. with a high remanence, which implies a high value of J_r/J_s), and suitable for practical purposes (i.e. having a small coercive force).

1) We have seen that if J_r/J_s is to be high, the crystal anisotropy must be predominant. A high value of $|K|$ implies a low value of μ_i , if μ_i originates only from rotational processes. The aim, then, is to produce a ferrite of fairly low initial permeability.

¹⁴ Thus $(1-p)$ is the ratio of the macroscopic (or apparent) density of the material to the microscopic (or true) density. The latter can be determined by X-ray diffraction methods, the former by the ordinary methods of density measurement.

At the same time it follows from formula (4) that the coercive force H_c increases with $|K|$, so that the crystal energy must not be so great that H_c assumes undesirably high values.

2) The porosity should be as small as possible; demagnetizing fields are then small and H_c will be smallest.

3) A small value of the magnetostriction in the preferred direction is favourable for squareness. Square-loop ferrites suitable for practical purposes, however, can be obtained only if the two first conditions are fulfilled. In the mixed-crystal systems referred to in figs. 5 and 6 this is not the case.

The frequency characteristics of the ferrite are also important. It is clear from the article I that a low value of μ_i will be accompanied by a high ferromagnetic resonance frequency: this is a primary requirement if the hysteresis loop is to be rectangular with pulses of about 1μ sec. It is also seen from I that it is just with those ferrites which have the smallest initial permeability that the irreversible Bloch-wall displacements are able to follow the current variations up to the highest frequencies. If difficulties due to eddy currents are to be avoided, moreover, the resistivity of the material must be sufficiently high. It appears to be not difficult to attain values higher than 10^3 or even 10^4 ohm metres (M.K.S. system), which means a factor of 10^9 to 10^{11} higher than that of metallic soft magnetic materials.

Examples of ferrites with rectangular hysteresis loops

Measurements of the hysteresis loop have been carried out with a ballistic galvanometer. The dependence of the results on the frequency will not be discussed here. Before considering the square loop materials, a brief review of some well-known materials will be given.

The porosity of Ferroxcube IIIB is about 10%. The coercive force and the crystal anisotropy are both low, and it can therefore be expected that the porosity will result in a considerably reduced value of J_r/J_* ¹⁵); in fact, an average value of 0.27 is obtained. Accordingly $\mu_{rem}/\mu_i = 0.96$. The squareness ratio is of course very small: $(R_s)_{max} \approx 0$.

Ferroxcube IVE has a higher coercive force ($\mu_0 H_c = 14 \times 10^{-4} \text{ Wb/m}^2$) and a larger crystal anisotropy (μ_i is only 17), both factors being favourable for a rectangular hysteresis loop. If this

material is fired at the normal temperature, however, it is very porous ($p = 25\%$), and the demagnetizing fields again become significant. It is found that $J_r/J_* < 0.6$; $\mu_{rem}/\mu_i = 0.63$, and $(R_s)_{max} = -0.15$. These values show an improvement when the material is fired at a higher temperature; the porosity is then only 10%. In this case, notwithstanding a decrease in coercive force (down to $\mu_0 H_c = 3 \times 10^{-4} \text{ Wb/m}^2$), the loop is more rectangular, viz. $J_r/J_* = 0.6$, $\mu_{rem}/\mu_i = 0.55$, and $(R_s)_{max} = 0.70$.

The chemical compositions and properties of a number of ferrites giving rectangular hysteresis loops, together with those of some other ferrites, are given in Table II. The relationship in sintered ferrites between μ_{rem}/μ_i and J_r/J_* can be seen from the table and from fig. 9. For low values of J_r/J_* , μ_{rem}/μ_i approximates to 1. For the maximum value that can be anticipated, viz. $J_r/J_* = 0.87$, the ratio μ_{rem}/μ_i should approach a value of 0.36, and this is roughly the case as shown in fig. 9. Striking results were obtained from the following ferrites.

1) $\text{Co}_{0.02}\text{Mn}_{0.48}\text{Fe}_2\text{O}_4$. The hysteresis loop of this ferrite is not particularly square, but the material has that advantage of a small coercive force: $\mu_0 H_c = 0.43 \times 10^{-4} \text{ Wb/m}^2$.

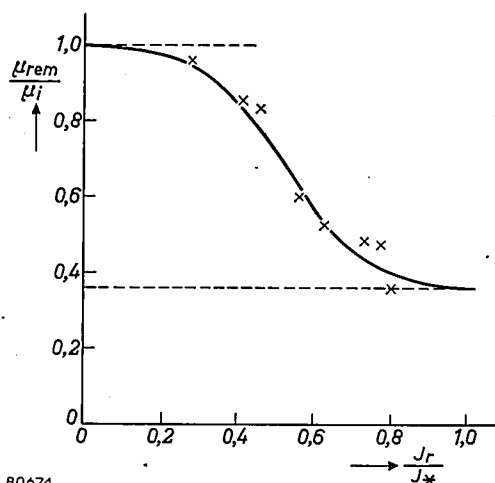


Fig. 9. Relationship between the quantities μ_{rem}/μ_i and J_r/J_* .

2) $\text{CuO}_{0.1}(\text{MnO}_{1+\delta})_{1.1}\text{Fe}_2\text{O}_3$ is remarkable for its low coercive force: $\mu_0 H_c = 0.67 \times 10^{-4} \text{ Wb/m}^2$.

3) $\text{MgO}_{0.5}(\text{MnO}_{1+\delta})_{0.875}\text{Fe}_2\text{O}_3$ is a very close-grained ferrite. Some idea of the porosity can be obtained from the photomicrograph of the polished surface shown in fig. 10a. For comparison fig. 10b shows a similar photograph of the porous Ferroxcube IIIA ($p=9\%$). From the table it is seen that $(R_s)_{max} = 0.81$, whilst $(J_0/J_{H_m})_{max} = 0.96$.

4) $\text{Mn}_{0.1}\text{Ni}_{0.5}\text{Mg}_{0.4}\text{Fe}_2\text{O}_4$. Porosity 5%. This ferrite has remarkably good characteristics, viz.

¹⁵ By J_* is meant the magnetization of a ring measured at $\mu_0 H = 0.01 \text{ Wb/m}^2$ ($H = \text{oersted}$). Since H_c is very much smaller, an adequate approximation to J_s is obtained by replacing it by the slightly smaller value J_* .

Table II. Properties of ferrites with rectangular hysteresis loops.

No.	Chemical composition	Porosity p %	μ_i	μ_{rem}/μ_i	J_r/J_*	$(J_0/J_{H_m})_{max}$	$(R_s)_{max}$	$\mu_0 H_c :$ 10^{-4} Wb/m ² $H_c :$ oersted	$\mu_0 H_m$ for $(R_s)_{max}$ 10^{-4} Wb/m ²
	Ferroxcube IIIB	10	1230	0.96	0.27	0.32	~ 0	0.8	
	Ferroxcube IVE, fired at 1250 °C	25	17	0.63	< 0.6	0.70	-0.15	14	
	„ „ 1450 °C	10	42	0.55	0.6		0.70	3	
1	$Co_{0.02}Mn_{0.48}Fe_2O_4$	6	83	0.86	0.41	0.83	0.59	0.43	0.48
2	$(CuO)_{0.1} \cdot (MnO_{1+\delta})_{1.1} \cdot Fe_2O_3$	3	86	0.56	0.60	0.93	0.76	0.67	0.85
3	$(MgO)_{0.5} \cdot (MnO_{1+\delta})_{0.875} \cdot Fe_2O_3$		55	0.49	0.73	0.96	0.81		1.35
4	$Mn_{0.1}Ni_{0.5}Mg_{0.4}Fe_2O_4$	5	138	0.48	0.76	0.95	0.83		1.7
5	$Mg_{0.4}Ni_{0.6}Fe_2O_4$		28	0.53	0.62	0.94	0.84		2.6
6	$Li_{0.46}Ni_{0.08}Fe_{2.40}O_4$	5	40	0.36	0.8		0.78		4.3
7	$Li_{0.25}Cu_{0.5}Fe_{2.25}O_4$	4					0.75		

$(J_0/J_{H_m})_{max} = 0.95$ and $(R_s)_{max} = 0.83$ with a field $\mu_0 H_m = 1.7 \times 10^{-4}$ Wb/m².

5) $Mg_{0.4}Ni_{0.6}Fe_2O_4$. The outstanding feature of this ferrite is that the squareness ratio is only very slightly dependent on the temperature. We shall return to this point later. It is found among the mixed crystals of Mg ferrite with Ni ferrite, that firing at 1450 °C does not always ensure low porosity; now and then a rectangular loop is obtained with $p = 20\%$. Microscopic examination of the polished surface gives the explanation: the high porosity is in this case due to much larger pores than in other ferrites. The initial permeability is low ($\mu_i = 28$).

6) $Li_{0.46}Ni_{0.08}Fe_{2.40}O_4$. It appears that "lithium ferrite" ($Li_{0.5}Fe_{2.5}O_4$) fired at 1000 °C in oxygen exhibits slightly negative magnetostriction. If it is chemically reduced by firing at a somewhat higher temperature (1150 °C) so that a mixed crystal of lithium ferrite and ferrous ferrite is produced, a positive magnetostriction in the pre-

ferred direction is obtained. Intermediate firing temperatures, give the greatest squareness but it is still insufficient for practical purposes because the relatively low temperature results in too much porosity. Firing at higher temperatures gives a lower porosity, but an increased ferrous ferrite content, and hence not a low magnetostriction. An improvement was obtained by starting with a mixed crystal of lithium and nickel ferrite. The apparent density of this material is 4.60, and the actual density of the material itself is 4.85. This, combined with a high value of $|K|$ (since $\mu_i = 40$) promotes squareness of the loop (see Table II).

7) $Li_{0.25}Cu_{0.5}Fe_{2.25}O_4$. Porosity 4%, $(R_s)_{max} = 0.75$.

As explained above, the squareness ratio R_s of a hysteresis loop is a function of the maximum field strength H_m at which the loop is measured. Fig. 11 shows R_s as a function of H_m for the ferrites listed in Table II. It is seen that the lower the field strength

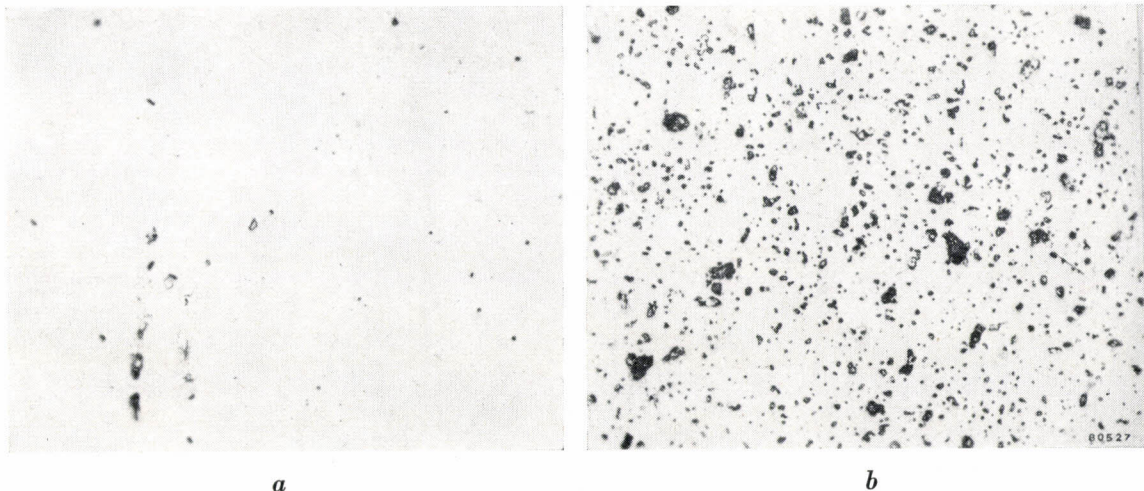


Fig. 10. Photo-micrographs of polished surfaces (magn. 400 \times). a) Ferrite No. 3 (Table II). b) Ferroxcube IVA. $p = 0.09$.

at which R_s reaches a maximum, the more R_s depends on H_m . The figure also shows the ratio J_0/J_{H_m} plotted against H_m . It may be noted that the optimum field for R_s is practically the same as for J_0/J_{H_m} .

Special properties

In many applications of square hysteresis loop ferrites a low temperature coefficient and high stability of the constants $(R_s)_{max}$ and $(J_0/J_{H_m})_{max}$

(except 40°C) a loop can be obtained which is more rectangular, corresponding to a different value of H_m , but it is found that the spread in $(R_s)_{max}$ within a certain range of temperatures is smallest for those loops which refer to the optimum field H_m for the average temperature (40°C) in the working range.

Stability of the hysteresis loop

Fig. 13 shows an ideal rectangular hysteresis

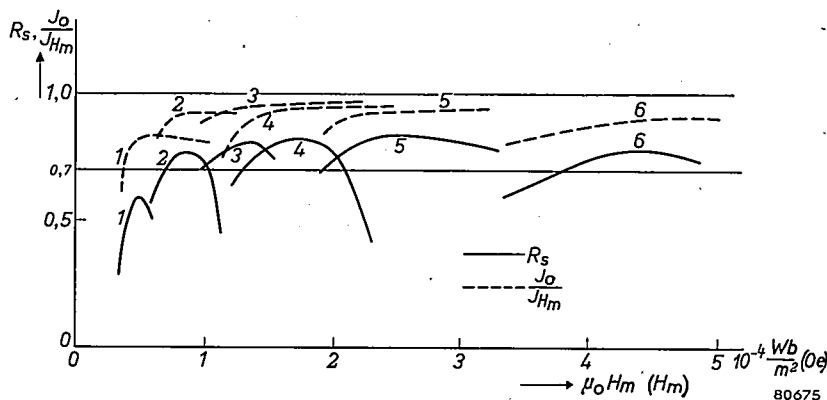


Fig. 11. R_s and J_0/J_{H_m} plotted against H_m for a number of the ferrites in Table II.

are also required. These factors will now be briefly reviewed.

Effect of temperature on $(R_s)_{max}$

Different meanings can be attached to the dependence of $(R_s)_{max}$ upon the temperature. We choose a temperature range of 20 to 60°C. in which R_s is determined in respect of values of H_m such that R_s at 40°C is equal to $(R_s)_{max}$. The values obtained for a number of ferrites are plotted in fig. 12 against the temperature. At any temperature

loop. It will be clear that if this loop be followed round a number of times to the point where $H = H_m$, this will be the point I in the diagram. When H is made zero, point II will be reached. A current pulse which causes H to drop to $-\frac{1}{2}H_m$ brings us to point III and, if H then again becomes zero, the material will return to the state represented by point II. In the applications for which this material is employed the cycle II-III-II may

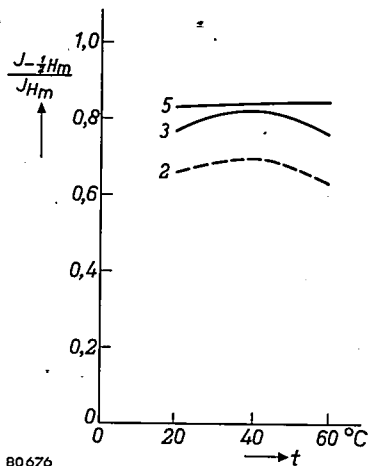


Fig. 12. R_s as a function of the temperature, for the three ferrites (2), (3) and (5) in Table II.

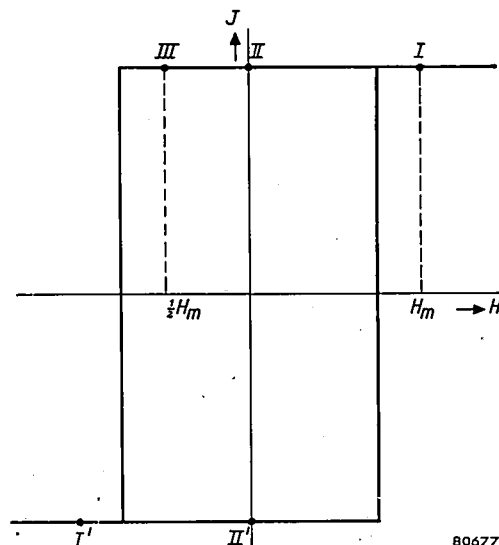


Fig. 13. Ideal rectangular hysteresis loop.

occur many times before a pulse of magnitude $-H_m$ arrives to bring the material into condition I' and then II' , i.e. to reverse the sign of the magnetization.

How far the non-ideal available materials approximate to this behaviour may be gathered from fig. 14. This shows one half of the hysteresis loop corresponding to the optimum squareness ratio for one quality of ferrite. The point I was measured after the field H_m had gone through a number of

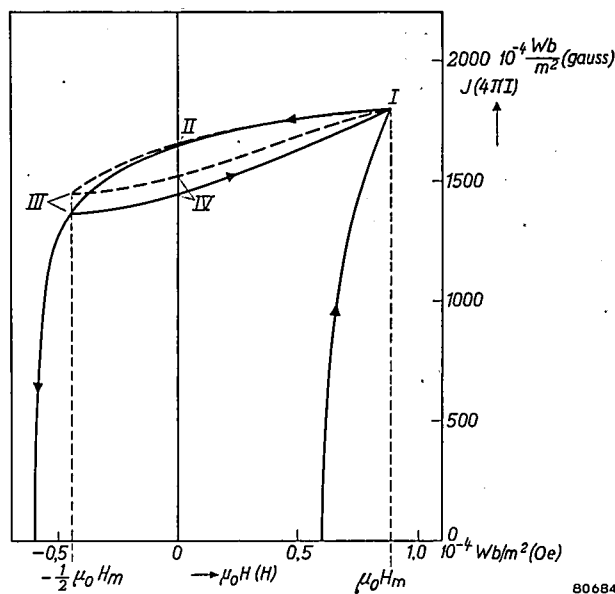


Fig. 14. Hysteresis loop of ferrite No. 2 (see Table II) when the field is varied a number of times from $H = H_m$ to $H = -\frac{1}{2}H_m$.

cycles. When H_m is removed the point II is reached. An opposing field $-\frac{1}{2}H_m$ gives point III and, when this in turn is removed, a point IV is reached which is lower than II . The variation of points $I - IV$ when the cycle $I-II-III-IV$ is completed a number of times has also been investigated. Ferrite No. 2 in Table II was used for this purpose. It was found that after a large number of cycles of the subsidiary loop $I-II-III-IV$, the induction at point I had dropped by less than 1%. Point II remained constant within experimental error; point III rose: the corresponding induction value may increase by more than 5%. Point IV also rose considerably. The final situation is that the subsidiary loop has moved to the position shown by the broken line in fig. 14. Clearly, the squareness ratio R_s does not diminish but even increases, in this case from 0.76 to 0.81.

Summary. For certain purposes (computing machines, switching elements) cores of magnetically soft material (i.e. with small coercive force) are required, having almost rectangular hysteresis loops. Ferrites fulfil these requirements and also have the advantage that eddy currents and other losses are only small when the field is varied rapidly. The shape of the hysteresis loop of ferrites is determined by the nature of the anisotropy governing the direction of the magnetization vector (crystal, stress or shape anisotropy). Pronounced crystal anisotropy is an advantage (and with it the accompanying low initial permeability μ_i), but it should not be so high that the coercive force becomes too great. In order to minimize the other kinds of anisotropy, internal strain and porosity should be avoided. A number of suitable ferrites especially developed for the purposes mentioned above are described and their properties enumerated.

MIRROR CAMERAS FOR GENERAL X-RAY DIAGNOSTICS

by W. HONDIUS BOLDINGH.

778.33:771.31:616-073.75

The use of fluorography is becoming more and more common and is now also employed in general X-ray diagnostics. Attempts to minimize the dosage to which the patient is exposed during this type of examination have developed along two quite separate lines, namely, the improvement of optical efficiency in photographic systems, and the use of electronic aids (e.g. the X-ray image intensifier) to increase the image luminance. It is difficult at the present stage to predict the ultimate relationship between the two methods; the former, however, has now attained a considerable measure of perfection. The present article describes some of the latest designs of the fluorographic cameras used.

Fluorography, that is, the photographing of fluorescent X-ray images with the aid of a camera instead of by direct contact with a film, was originally developed for mass chest survey. The merits of the method as applied to this particular branch of diagnostics have been discussed fully in earlier issues of this Review^{1) 2)}. All that we need

recall here is that documentation is thus achieved without undue expense of film and filing space, and

- 1) A. Bouwers and G. C. E. Burger, X-ray photography with the camera, Philips tech. Rev. 5, 258-263, 1940.
- 2) H. J. di Giovanni, W. Kes and K. Lowitzsch, A transportable X-ray apparatus for mass chest survey, Philips tech. Rev. 10, 105-113, 1948/1949.